

SELF-ORGANISATION OF GAIT PATTERN TRANSITION

An Efficient Approach to Implementing Animal Gaits and Gait Transitions

Zhijun Yang, Juan Huo and Alan Murray

*Institute of Micro and Nano Systems, School of Engineering and Electronics
Edinburgh University, Edinburgh EH16 6XD, U.K.
{Zhijun.Yang, J.Huo, Alan.Murray}@ed.ac.uk*

Keywords: Central pattern generator, oscillatory building block, gait transitions, Self-organisation, Hopfield network.

Abstract: As an engine of almost all life phenomena, the motor information generated by the central nervous system (CNS) plays a critical role in the activities of all animals. Despite the difficulty of being physically identified, the central pattern generator (CPG), which is a concrete branch of studies on the CNS, is widely recognised to be responsible for generating rhythmic patterns. This paper presents a novel, macroscopic and model-independent approach to the retrieval of different patterns of coupled neural oscillations observed in biological CPGs during the control of legged locomotion. Based on the simple graph dynamics, various types of oscillatory building blocks (OBB) can be reconfigured for the production of complicated rhythmic patterns. Our quadrupedal locomotion experiments show that an OBB-based artificial CPG model alone can integrate all gait patterns and undergo self-organised gait transition between different patterns.

1 INTRODUCTION

Animal gait analysis is an ancient science. As early as two thousand years ago, Aristotle described the walk of a horse in his treatise (Aristotle, 1936). In modern biological research, it is widely believed that animal locomotion is generated and controlled, in part by central pattern generators (CPG), which are networks of neurons in the central nervous system (CNS) capable of producing the rhythmic outputs (Stein, 1978),(Grillner, 1985),(Pearson, 1993). The constituents of the locomotory motor system are traditionally modelled by nonlinear coupled oscillators, representing the activation of flexor and extensor muscles by, respectively, two neurophysiologically simplified motor neurons (Linkens et al., 1976),(Tsutsumi and Matsumoto, 1984),(Bay and Hemami, 1987). Despite its mathematical accuracy and ability to mimic some basic oscillatory features, this approach provides, however, neither a sufficiently detailed description of the real biological mechanisms nor a model simple enough for application purpose. Based on the graph dynamics, in this paper we present a structural approach to the modelling of the complex behavioural dynamics with a new concept of oscillatory building blocks (OBB) (Yang and Franca, 2003), (Yang and Franca, 2008). For the first time we present that the OBB model is able to self-organise its dif-

ferent gait pattern outputs under the control of a selecting signal flow in the neuro-musculo-skeletal system. Through appropriate selection and organisation of suitably configured OBB modules, different gait patterns and transitions between different patterns can be achieved for producing complicated rhythmic outputs, retrieving realistic locomotion prototypes and facilitating the very large scale integrated (VLSI) circuit synthesis in an efficient, uniform and systematic framework.

2 METHOD

Out-of-phase (walking and running) and in-phase (hopping) are the major characteristics of observed gaits in bipeds, while in quadrupeds more gait types were observed and enumerated (Alexander, 1984), as walk, trot, pace, canter, gallop, bound and pronk. Unlike bipeds and quadrupeds, hexapod locomotion can have more complicated combinations of leg movements. Despite the variety, however, some general symmetry rules should still be obeyed and remained as the basic criteria for gait prediction and construction. For instance, it is a generally accepted view that multi-legged (usually more than six legs) locomotion often display a travelling wave sweeping along the chain of oscillators (Collins and Stewart, 1993),(Gol-

ubitsky et al., 1998). In order to construct a novel, uniform OBB-based CPG architecture to integrate all gaits as well as the self-organised gait transitions of a specific legged animal, we need a case study of the simple graph dynamics as a start.

2.1 A Case of Graph Dynamics

Consider a system consisting of a set of processes and a set of atomic shared resources represented by a connected graph $G = (N, E)$, where N is the set of processes and E the set of edges defining the interconnection topology. An edge exists between any two nodes if and only if two corresponding processes share at least one atomic resource (Fig. 1).

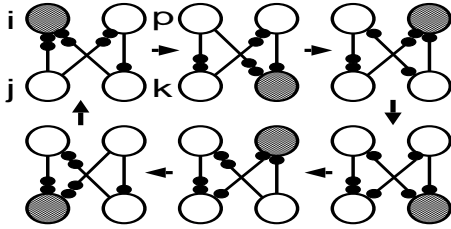


Figure 1: A simple graph dynamics representing an operation cycle, $r_i = r_j = 2$, $r_k = r_p = 1$, dark-filled circle represents a node is operating.

Between any two nodes i and j , $i, j \in N$, there can exist e_{ij} unidirected edges, $e_{ij} \geq 0$. The reversibility of node i is r_i , i.e., the number of edges that shall be reversed by i to each of its neighbouring nodes, indiscriminately, at the end of the operation. Node i is an r_i -sink if it has at least r_i edges directed to itself from each of its neighbours. Only r_i -sink node can operate and reverse r_i edges towards each of its neighbours, the new set of r_i -sinks will operate, and so on. In order to avoid operation deadlock, the shared resources between any two nodes, e_{ij} , must satisfy $e_{ij} = r_i + r_j - \gcd(r_i, r_j)$, and $\max\{r_i, r_j\} \leq e_{ij} \leq r_i + r_j - 1$ (Barbosa, 1996), where \gcd for the greatest common divisor. This simple graph dynamics can be used to construct the artificial CPGs by implementing OBB modules as asymmetric Hopfield-like networks, where operating sinks can be regarded as firing neurons in purely inhibitory neuronal networks.

2.2 Dynamics of an OBB Module

An OBB module is defined to have a pair of r_i -sink and r_j -sink nodes, n_i and n_j , sharing the number of e_{ij} resources. The postsynaptic membrane potential of neuron i at t instant, $M_i(t)$, depends on three factors, i.e., the potential at the last instant $M_i(t-1)$, the impact of its coupled neuron output $v_j(t-1)$, and the

negative feedback of neuron i itself $v_i(t-1)$, without considering the external impulse. The selection of system parameters, such as the neuron thresholds and synapse weight, are crucial for modelling. In our model, let $r = \max(r_i, r_j)$ and $r' = h(r)$, where h is a function of highest integer level and multiplying it by 10, e.g., if $r_i = 81$ and $r_j = 341$ then $r' = h(r) = h(\max(81, 341)) = h(341) = 10^3$. We can further design neuron i and j 's thresholds θ_i , θ_j and their synapse weights w_{ij} , w_{ji} as follows,

$$\begin{cases} \theta_i = \max(r_i, r_j) / (r_i + r_j - \gcd(r_i, r_j)) \\ w_{ij} = \max(r_i, r_j) / r' \\ \theta_j = (\min(r_i, r_j) - 1) / (r_i + r_j - \gcd(r_i, r_j)) \\ w_{ji} = \min(r_i, r_j) / r' \end{cases} \quad (1)$$

The difference equation in the discrete time domain of this system can be formulated as follows: each neuron's self-feedback strength is $w_{ii} = -w_{ij}$, $w_{jj} = -w_{ji}$. The activation function is a sigmoidal Heaviside type. It is worth noticing that k is a local clock pulse of each neuron, a global clock is not required. Thus we have,

$$\begin{cases} M_i(t+1) = M_i(t) + w_{ji}v_j(t) + w_{ii}v_i(t) \\ M_j(t+1) = M_j(t) + w_{ij}v_i(t) + w_{jj}v_j(t) \end{cases} \quad (2)$$

where,

$$\begin{cases} v_i(t) = \max(0, \text{sgn}(M_i(t) - \theta_i)) \\ v_j(t) = \max(0, \text{sgn}(M_j(t) - \theta_j)) \end{cases} \quad (3)$$

We consider the designed circuit as a conservative dynamical system in an ideal case. The total energy is constant, no energy loss or complement is allowed. The sum of two neurons' postsynaptic potential at any given time instant is normalised to one. It is clear that this system has the capability of self-organised oscillation with the firing rate of each neuron arbitrarily adjustable.

If a neuron has more than one connections, then its firing state depends on the interactions of all the connections,

$$V_i(t) = \prod_{j=1}^n v_i^j(t) \quad (4)$$

For instance, neuron i in Fig. 1 has connections with both neuron j and k , the output of i is expressed as $V_i(t) = v_i^j(t) \times v_i^k(t)$, here $v_i^j(t)$ and $v_i^k(t)$ are obtained from the above dynamical equations.

3 QUADRUPEDAL GAIT MODEL

Generally seven types of primary gait patterns are identified for a quadruped in literature (Alexander,

1984). These can be summarised in Table 1.

Table 1: Quadrupedal primary gaits and description.

Gaits	Pattern description	
	Ipsilateral legs	Contralateral legs
walk	quarter cycle out	half cycle out
trot	half cycle out	half cycle out
pace	in phase	half cycle out
gallop	half cycle out	quarter cycle out
bound	half cycle out	in phase
pronk	in phase	in phase
jump	quarter cycle out	in phase

The proposed CPG model, with adaptable, different model parameters, is able to generate all the gait patterns shown in Table 1. The signals selecting gaits and controlling transitions in the CPG, usually in the spinal cord, come from the higher neural level in the prefrontal, premotor and motor cortices following the dog's interaction with its environment.



Figure 2: Trot gait of a dog.

We choose a dog's risk-avoiding behaviour to build a case study of an CPG model which is made of the OBB modules. Suppose a dog is initially wandering around in a walk gait. Suddenly it is frightened by something and makes an abrupt left turn and escapes with a faster trot gait (Fig 2). In this scene the dog's trajectory includes three different stages in sequence: walk, left turn (a special gait) and trot. These locomotion behaviours are controlled by the different motor driving outputs from its CPG. The activity of a dog's leg is simplified and generated by the activity of a flexor and an extensor motor neuron, respectively. The firing of a neuron in the OBB drives the flexor which lifts the leg from the ground in a swing stage. The idleness of a neuron activates the extensor which lands the leg on the ground in a stance stage.

The OBB network topologies for the rhythmic pattern generation, and the phase relationship for aforementioned three gait patterns are shown in Fig 3, where the firing cell (gray colour) denotes its corresponding leg is lifting from the ground. In the right, black-white bar, black bars specify the firing of flexors while white ones for the firing of extensors. It is clear that the special, left turn gait has a gait pattern

circulation as shown in Fig. 1.

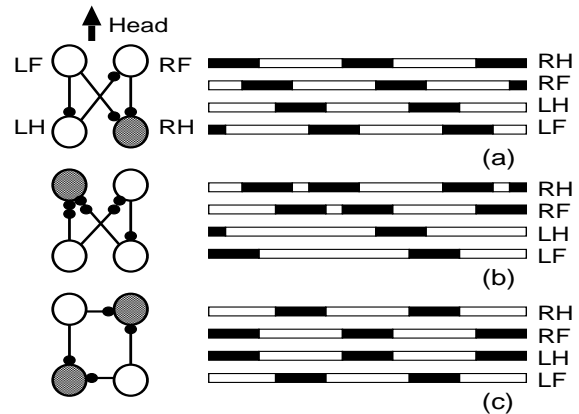


Figure 3: The schematic diagram of three gaits and their phase relations. The little black circles denote the shared resources, gray cells are firing and white ones are idle. The left side topology is only one configuration of a circulation period of a pattern. RF - right front, RH - right hind, LF - left front, LH - left hind. (a) walk, (b) left turn, (c) trot. .

From the biological knowledge we know that locomotion speed is decided by both the coordinated phase relation among legs and the duty factor, which is the proportion of an extensor's firing duration in one period. When an animal's locomotion speed increases, the extensor firing time (corresponding to stance) will decrease drastically while the flexor firing time (to swing) keeps basically constant (Pearson, 1976). This results in a lower duty factor, a relatively longer swing stage and a faster locomotion speed. As the same with adjusting coordinated phase relationship, the duty factor can also be modified by changing the reversibilities of two coupled cells.

4 SIMULATION RESULTS

A schematic circuit diagram of OBB-based asymmetric Hopfield-like neural network is shown in Fig. 4. A computer simulated example of quadruped risk-avoiding behaviour is conducted using this network and the pre-defined cell reversibilities. There are totally six possible connections between any two cells in this CPG architecture (as shown in Fig. 3), among which four connections are selected for a given gait pattern. The selecting signals, labelled from a_1 to a_6 , control the selection of an individual connection, respectively, and come from the higher cortex. The change of these signals denotes a change of connection topology. This change, together with the change of reversibilities of the cells, decides the transition of gait patterns.

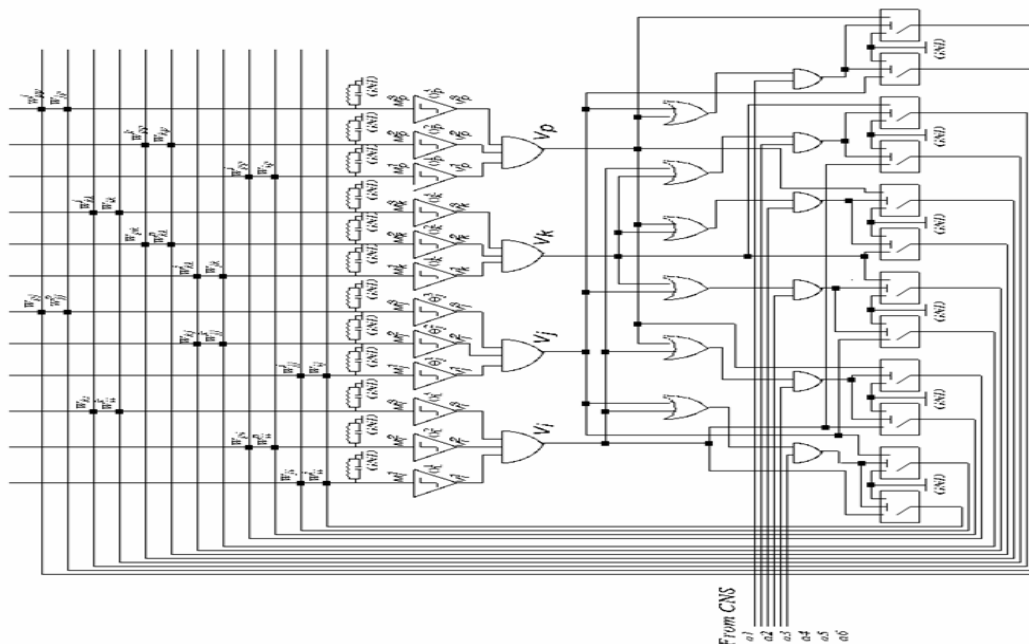


Figure 4: Quadraped CPG architecture. The cell output V_i , V_j , V_k , V_p correspond to LF, LH, RH, RF respectively. The predefined cell reversibilities are $r_i = r_j = r_k = r_p = 1$ for the walk and trot gaits, $r_i = r_j = 2$ and $r_k = r_p = 1$ for the left turn gait. The initial membrane potentials are $M_i^j(0) = M_i^k(0) = M_j^p(0) = M_k^k(0) = M_k^j(0) = 0.45$, $M_j^i(0) = M_k^i(0) = M_p^p(0) = M_p^j(0) = M_p^k(0) = 1.05$, $M_i^p(0) = 0.55$, $M_p^i(0) = 0.95$. The gait select signals are $[a1, a2, a3, a4, a5, a6] = [111001]$ for walk and trot, $[001111]$ for left turn. The cell thresholds and weights follow equation 1.

An array of twelve comparators, three for a cell, is used to compare the sub-cells' membrane potentials with thresholds. If a connection is absent then the relative comparator is disabled. The enabled connections of a cell converge to an AND gate, to implement equation 4 for the cell output. If a cell has an output, this output will make three OR gates, corresponding to its connections with all rest cells, have an output. These OR gate outputs are selected by the control signals from CNS at an array of AND gates, whose values are fed to an array of swithes, and form a loop to the input weight matrix for the comparator array.

According to equation 4, The output of a cell is the multiplication of two terminal outputs connecting with the cell's two neighbours. A cell will fire if and only if its sub-cells are firing simultaneously. An additional control (not shown) is needed to ensure that all shared resources on an edge will not reverse unless the output of a cell is firing. The system parameters are given in the legend of Fig. 4. The choice of initial membrane potential for every sub-cells is to make all cells work, i.e., being firing or idle, in an appropriate configuration of a starting gait's circulation period. After the choice of the membrane potentials the system will run adaptively in its gait transition which is controlled by the CNS signals. There

is a self-organisation period observable in Fig. 5 from walk to left turn gait. Another self-organisation between left turn to trot should exist whose effect may be minimised if the system parameters are occasionally appropriate for the next locomotion pattern at the transition time instant.

5 CONCLUSIONS

We have presented a novel central pattern generator model capable of generating a whole range of legged locomotion gait patterns. This CPG architecture is generalisable to mimic any gait patterns of any legged animals from biped to centipede. Self-organisation in gait transition is observed in control of a limited number of signal flow bits from the high level cortex. This modular system is simple and highly compatible to circuit implementation.

ACKNOWLEDGEMENTS

This work is supported by a British EPSRC grant EP/E063322/1, a Chinese NSF grant 60673102 and

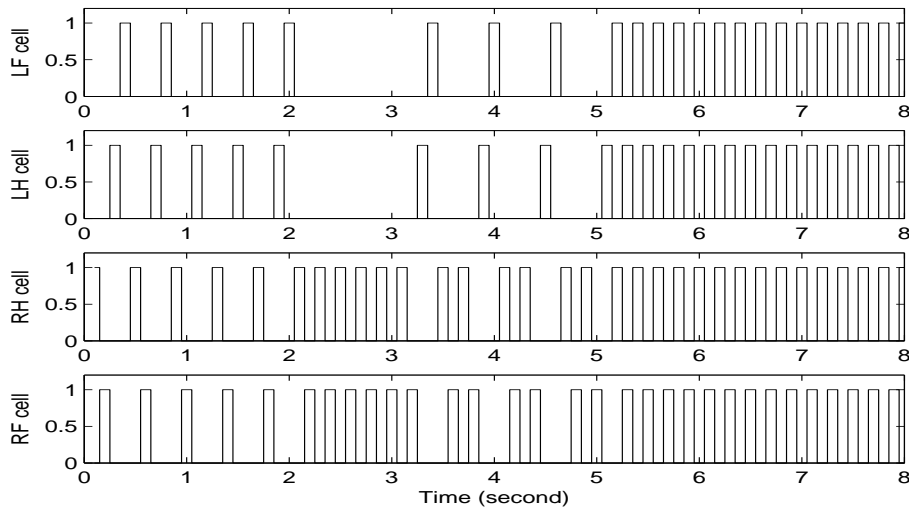


Figure 5: Cell output. Cell activity is equivalent to flexor activity and contrary to extensor activity in phase. The virtual dog starts with walk for 2 seconds. After that the left turn gait lasts for 3 seconds, which include a one-second self-organisation period. From the fifth second on it uses the faster trot gait to avoid the risk.

a Jiangsu Province grant BK2006218. We thank the useful discussions with Dr. Felipe M.G. Franca and Mr. Rodrigo Rodvalho.

REFERENCES

- Alexander, R. (1984). The gait of bipedal and quadrupedal animals. *Intl J. Robotics Research*, 3:49–59.
- Aristotle (Translated version of 1936). *On Parts of Animals, Movement of Animals, Progression of Animals*. By A.S. Peek and E.S. Forster (translators). Cambridge, MA: Harvard University Press.
- Barbosa, V. (1996). *An introduction to distributed algorithms*. Cambridge, MA: The MIT Press.
- Bay, J. and Hemami, H. (1987). Modeling of a neural pattern generator with coupled nonlinear oscillators. *IEEE Trans. Biomedical Engr.*, 34:297–306.
- Collins, J. and Stewart, I. (1993). Coupled nonlinear oscillators and the symmetries of animal gaits. *Journal of Nonlinear Science*, 3:349–392.
- Golubitsky, M., Stewart, I., Buono, P., and Collins, J. (1998). A modular network for legged locomotion. *Physica D*, 115:56–72.
- Grillner, S. (1985). Neurobiological bases of rhythmic motor acts in vertebrates. *Science*, 228:143–149.
- Linkens, D., Taylor, Y., and Duthie, H. (1976). Mathematical modeling of the colorectal myoelectrical activity in humans. *IEEE Transactions on Biomedical Engineering*, 23:101–110.
- Pearson, K. (1976). The control of walking. *Scientific American*, 235:72–86.
- Pearson, K. (1993). Common principles of motor control in vertebrates and invertebrates. *Annual Review of Neuroscience*, 16:265–297.
- Stein, P. (1978). Motor systems with specific reference to the control of locomotion. *Annual Review of Neuroscience*, 1:61–81.
- Tsutsumi, K. and Matsumoto, H. (1984). A synaptic modification algorithm in consideration of the generation of rhythmic oscillation in a ring neural network. *Biological Cybernetics*, 50:419–430.
- Yang, Z. and Franca, F. (2003). A generalized locomotion cpg architecture based on oscillatory building blocks. *Biological Cybernetics*, 89:34–42.
- Yang, Z. and Franca, F. (2008). *A general rhythmic pattern generation architecture for legged locomotion*, In *Advancing artificial intelligence through biological process applications* (A. Porto, A. Pazos, W. Buno, editors). Hershey, PA: Idea Group Inc.